Bioactive Materials 38 (2024) 411–421

Contents lists available at ScienceDirect

Bioactive Materials

journal homepage: www.keaipublishing.com/en/journals/bioactive-materials

Thrombogenicity of biodegradable metals

D.E.J. Anderson [a,*], H.H. Le [a], H. Vu [a], J. Johnson [a], J.E. Aslan [b], J. Goldman [c], M.T. Hinds [a]

[a] Department of Biomedical Engineering, Oregon Health & Science University, Portland, OR, USA
[b] Knight Cardiovascular Institute, Oregon Health & Science University, Portland, OR, USA
[c] Department of Biomedical Engineering, Michigan Technological University, Houghton, MI, USA

ARTICLE INFO

Keywords:
Vascular stents
Biodegradable metals
Thrombosis
Contact pathway
Platelets

ABSTRACT

Biodegradable metals offer a promising means to ameliorate many of the long-term risks associated with vascular devices made of conventional biostable stent metals. While numerous biodegradable metal alloys have been developed and characterized in animal models, knowledge of their blood reactivity and thrombogenicity remains unknown. Metal hemocompatibility is particularly valuable because current generation drug-eluting stents pose a significant long-term thrombosis risk. In this study, four pure metals, widely used as degradable base materials (Fe, Zn, Mg, and Mo), and three alloys commonly used in cardiovascular devices [NiTi, CoCr, and stainless steel (SS)] were evaluated. This work examined how each of these metals activate platelets, coagulation factors, and inflammation using *in vitro* hemocompatibility assays and a clinically relevant *ex vivo* non-human primate arteriovenous shunt model. Testing found that while all metals promoted a downstream activation of platelets and coagulation in flowing whole blood, platelet and fibrin attachment to Mg was markedly reduced. Additionally, Fe and Mo trended toward higher platelet attachment and contact pathway activation. Overall, the results suggest that Mg may delay clot initiation, but not eliminate clot formation, indicating the importance of understanding thrombosis in Mg alloys that are currently being developed for clinical use as biodegradable stents.

1. Introduction

Vascular diseases are the leading causes of morbidity and mortality globally [1]. Metal stenting is a common and increasingly used intervention to re-establish patency of blood vessels [2,3]. However, current bare metal biostable stents composed of stainless steel (SS) or cobalt chromium (CoCr) often failed to retain long-term patency due to neointimal hyperplasia causing vessel restenosis [4]. Consequently, drug eluting stents (DES) were developed to prevent restenosis by directly applying cytostatic agents at the site of vascular stenosis. These stents improved clinical outcomes in the first year after implantation [5], but the cytostatic agents also prevented reendothelialization, potentiating late-stage thrombosis and long-term chronic inflammation in DES implanted vessels [6]. Advances in antiplatelet therapies reduced the risk of stent thrombosis, but subjected patients to lifelong antithrombotic therapies—increasing bleeding risks and requiring close monitoring and additional management during secondary procedures [7,8]. Biodegradable polymer stents, including Abbott's Absorb™ stent, were subsequently developed to prevent the long-term need for antiplatelet and antithrombotic therapies. However, polymer stents generally exhibit insufficient radial strength, poor radio-opacity, and technical challenges in deployment and manufacturing [9]. The Absorb™ stent is no longer marketed, and follow up clinical studies showed a higher, although not statistically significant incidence of stent thrombosis [10]. Thus, biodegradable metallic stents have emerged as an alternative to meet both the mechanical and biological requirements of vascular stents while mitigating the long-term thrombotic or inflammatory risks of permanent stents.

Biodegradable metals present an excellent opportunity for cardiovascular devices, specifically alloys of Mg, Fe, and Zn have been used as based materials for stenting [11]. Considerable work has produced a spectrum of various alloys with improved corrosion and mechanical properties compared with the unalloyed metal [11,12]. However, far less work has investigated the biological healing responses invoked by the presence of these metals in the arterial environment. Despite advances in interventional cardiology [13–16] and anti-thrombotic therapies [17,18], the widely used vascular stents, including DES, still have high rates of thrombosis and restenosis from intimal hyperplasia with

Peer review under responsibility of KeAi Communications Co., Ltd.
* Corresponding author.
E-mail address: anderdei@ohsu.edu (D.E.J. Anderson).

https://doi.org/10.1016/j.bioactmat.2024.05.002
Received 21 December 2023; Received in revised form 10 April 2024; Accepted 2 May 2024

severe clinical consequences [19–21]. As reviewed elsewhere [22], early stent thrombosis with bare metals stents occurs in up to 16% of cases, and while that rate has improved with better anticoagulant and antiplatelet medications, late-stage thrombosis remains an issue with DES requiring some patients to remain on anticoagulants for months and years. This long-term requirement for anticoagulants is particularly concerning in the cases of 1) the need for invasive surgery and 2) flow diverting stents for brain aneurysms where anticoagulants are risky and contraindicated, respectively. While the need for antiplatelet and anticoagulant therapies will likely persist, it is critical to understand the mechanisms of material thrombogenicity in the absence of anticoagulants or antiplatelet therapies using clinically relevant models. Deeper understanding of metal and device specific risks will inform disease management and treatment guidelines, improving treatment regimens and reducing morbidity and mortality. Furthermore, degradable metal stents, which demonstrate resistance to thrombosis, may improve prognoses and outcomes.

Degradable metals break down into several soluble and insoluble byproducts, including the soluble metal ion of the base metal, and alter the pH of the physiological fluids at the implant surface [23]. Many of these metal ions are biochemically active within the cells and tissues of the arterial environment [24]. They are readily able to enter cells where they bind proteins and alter their structure and function [25]. For instance, previous work found that ionic Zn, at the concentrations present at the surface of a degradable pure Zn arterial implant, can activate cellular apoptotic signaling pathways, including caspase-3 [26], within neointimal smooth muscle cells near the implant surface, thereby beneficially reducing the presence and activity of these cells within the encapsulating neointimal tissue. Other biodegradable implants that include alloying elements have been found to elicit a wide spectrum of neointimal and inflammatory responses [11,27–31]. These responses may be impacted by the specific corrosion byproducts and their concentrations, degradation rates, and microstructural properties of these diverse biodegradable materials. Previous work also found that the surface properties of biodegradable metals influence their biocompatibility [32,33]. The generation of potentially bioactive byproducts at high local concentrations and an actively changing biointerface contribute to the complexity of biodegradable implants and the local cellular and tissue level responses relative to the conventional biostable stent metals.

To investigate thrombogenicity, this work quantified the hemocompatibility of the pure metals (Mg, Zn, Fe, and Mo) that are of interest in designing biodegradable stents. These results set a baseline for alloy testing and development. For comparison, commonly used clinical alloys [nitinol (NiTi), CoCr, and SS] were tested. The goal of these studies was to comparatively evaluate candidate metals with regard to acute pathways involved in thrombosis, including contact pathway activation, platelet attachment and activation, fibrin accumulation, and immunogenicity on metal wire constructs. The experiments quantified the biomaterial-initiated blood response *in vitro* through factor (F)XIIa generation and fibrin generation assays, using human plasma. FXII activation is a critical early step in the contact pathway activation branch of the coagulation cascade, while fibrin generation is the culmination of the common pathway of coagulation. These studies also used a strict, non-human primate (NHP) *ex vivo* thrombosis model of whole, flowing blood without antiplatelet or anticoagulant therapies to both quantify platelet and fibrin accumulation on the wires and measure critical thrombosis markers in the blood after exposure to the metal wires. The blood plasma was used to quantify platelet activation markers, including platelet factor 4 (PF4), soluble glycoprotein VI (sGPVI), and P-selectin, contact pathway markers including thrombin-antithrombin complexes (TAT), and immune activation including myeloperoxidase (MPO) release and platelet-leukocyte aggregates (PLAs). These results will inform the design and implantation parameters of clinically useful biodegradable metals for use in blood-contacting medical devices.

2. Materials and methods

2.1. Materials

Pure and alloyed metal wires (Goodfellow Corp., Pittsburgh, PA, Supplemental Fig. 1 for SEM imaging of untreated wires) were cut into straight lengths for *in vitro* testing or coiled around a 4 mm Teflon rod for *ex vivo* testing. The specific metals were Fe (99.99%, annealed, 0.25 mm diameter), Zn (99.99%, as drawn, 0.25 mm diameter), Mo (99.95%, annealed, 0.25 mm diameter), Mg (99.9%, as drawn, 0.25 mm diameter), SS (Fe/Cr18/Ni10/Mo3, as drawn, 0.25 mm diameter), CoCr (Co40/Cr20/Fe15/Ni15/Mo 7/Mn 2/C/Be, hard temper, 0.25 mm diameter), and NiTi (Ni55/Ti45, as drawn, 0.23 mm diameter). All wires were sonicated in 200 proof ethanol for 10min prior to testing and stored in ethanol to prevent corrosion.

2.2. In vitro coagulation testing

In vitro testing was performed, based on previous work [34,35], with protocol modifications for the metal wires, described in detail below.

2.2.1. Blood component isolation

Pooled platelet poor plasma (PPP) was isolated from healthy, human volunteers, as approved by the Oregon Health & Science University Institutional Review Board and described previously [36]. Briefly, whole blood was drawn into sodium citrate (3.2% w/v at a 1:10 ratio with the blood) and centrifuged to isolate a platelet pellet and PPP (once at 200*g* for 20min and once at 1000*g* for 10min with 0.1 μg/mL prostacyclin). PPP was aliquoted and stored at −80°C until use.

2.2.2. FXII activation assay

Straight wire lengths of 6 mm were placed in non-tissue culture treated 96-well plates for *in vitro* testing and rinsed briefly with 1X phosphate buffer saline (PBS). Conversion of FXII to FXIIa was quantified on the wires using pooled human PPP. The PPP was warmed to 37°C and added to each sample, followed by the addition of equal parts HEPES buffer (25 mM HEPES, 125 mM NaCl, pH 7.4) and chromogenic substrate (S-2302™, Diapharma, West Chester Township, OH). Samples were immediately read on a plate reader (Infinite M200 spectrophotometer, Tecan, Männedorf, Switzerland) using absorbance at 405 nm every 1min for 1hr at 37°C. The generated data curves were used to determine FXIIa generation from the maximum slope of the curve. Three wires were tested on three separate occasions for a total of n = 9, with a plasma only negative control.

2.2.3. Fibrin clotting assay

Straight wire lengths of 6 mm were placed in non-tissue culture treated 96-well plates for *in vitro* testing and rinsed briefly with PBS. Pooled human PPP was warmed to 37°C and added to each sample, followed by the addition of equal parts PBS with 25 mM $CaCl_2$. Samples were immediately read on a plate reader (Infinite M200 spectrophotometer, Tecan) using absorbance at 405 nm every 1min for 1hr at 37°C. The generated data curves were used to determine fibrin clotting time from the time at which the curve deviated from the baseline by 10% and fibrin clotting rate from the maximum slope of the curve. Three wires were tested on three separate occasions for a total of n = 9, with a plasma only negative control.

2.3. Whole blood shunt study

Animal studies were approved by the Oregon National Primate Research Center (ONPRC) Institutional Animal Care and Use Committee. Animals received full time care from the staff at ONPRC and work followed the guidelines from the National Research Council and the Committee on Care and Use of Laboratory Animals of the Institute of Laboratory Animal Resources.

2.3.1. Platelets and fibrin quantification using radiolabeling

For *ex vivo* testing, 12.7 cm length wires were coiled around a 4 mm outer diameter rod to a final length of approximately 2 cm (Fig. 1A). NiTi wires were heated over an open flame prior to coiling to reset the shape. All coils were contained within fluorinated ethylene propylene (FEP, Zeus Inc., Orangeburg, SC) heat shrink tubing—shrunk to a 4 mm outer diameter rod. The 2 cm length coils were placed into an exteriorized arteriovenous shunt loop made of Silastic tubing (4 mm ID, Dow Chemical) and exposed to flowing, whole blood testing without any anticoagulant or antiplatelet therapies (Fig. 1B). These NHP shunts were performed in three healthy, juvenile male *papio anubus* baboons (11.2–13.1 kg) based on a well-established thrombosis model [35, 37–43]. In brief, coils were exposed to whole, non-anticoagulated blood and blood flow was controlled at 100 mL/min for 1hr using a clamp distal to the coils, followed by a saline rinse. Dynamic platelet and endpoint fibrin attachment were quantified using radioisotopes, 111-In and 125-I, respectively (n = 6). The autologous platelets accumulated on the wires and were measured every minute with a Brivo NM615 (General Electric, Boston, MA). After decay of the 111-In isotope, fibrin was measured with a 1480 Wizard gamma counter (PerkinElmer, Waltham, MA).

2.3.2. SEM for qualitative assessment of thrombus

Shorter segments (2 cm) of the metal wires were inserted into the shunt loop approximately 0.8 m downstream of the coil for parallel testing with 1hr of flowing, whole blood (n = 2). These samples were straight wire segments placed longitudinally along the 4 mm inner diameter Silastic tubing with 2 cm segments of the FEP tubing inserted into either end to secure the wire. After the 1hr of blood flow and saline rinse, these samples were rinsed thoroughly with PBS, fixed in 3.7% paraformaldehyde (PFA) overnight at 4°C, and dehydrated with incubations of increasing concentrations of ethanol. Samples were stored in 200 proof ethanol then further dehydrated in hexamethyldisilazane (HMDS, Sigma, St. Louis, MO). After evaporation of the HMDS, samples were mounted onto SEM studs with carbon tape and sputter coated with platinum (ACE600 Leica). Samples were imaged using a Volumescope 2 SEM (Thermo Scientific, Waltham, MA) using high vacuum.

2.3.3. Downstream blood sampling

Boundary layer blood draws from 1 cm ± 2 mm downstream of the metal coils were collected based on a previously verified method [41, 43]. A continuous blood draw was pulled downstream of the metal coils into 10% by volume citrate at 1.5 mL/h, while PPACK (0.5 mg/mL Sigma) was infused (0.3 mL/h) just upstream of the blood draw to avoid occlusion of the blood draw tubing (Fig. 1B). This technique was shown to give a more concentrated solution of blood components that interacted with the surface of the biomaterial [43]. An initial blood draw was taken as a bulk draw (not boundary layer) and considered time 0min. The boundary layer blood draws were taken from 0 to 30min (hereafter labelled "30min") and from 30 to 60 (labelled "60min"). These blood draws were used for quantification of platelet and inflammation markers with flow cytometry (described below). Plasma was isolated from the remaining blood that was collected from the concentrated boundary layer by centrifugation for 3min at 10,000 RPM. This plasma was used for the biochemical assays and quantification of metal ions with inductively coupled plasma mass spectrometry (ICP-MS).

2.3.4. ICP-MS for metal degradation ions

Boundary layer PPP from the biodegradable metal experimental runs was tested for Mg, Fe, Zn, and Mo metal ions using ICP-MS (Agilent 7700x, Santa Clara, CA) at each of the three time points (n = 3). Elemental analysis was performed at the OHSU Elemental Analysis Core.

2.3.5. Flow cytometry

Whole blood, diluted at a factor of 1:4 with HEPES/Tyrodes (HT) buffer, was stimulated with platelet glycoprotein VI agonists, cross-linked collagen-related peptide (CRP-XL) at 0, 0.1, or 1 μg/mL CRP-XL and incubated with CD62-PE (BD Biosciences, Franklin Lakes, NJ) for 20min at 37 °C. For PLA analysis, 1:4 diluted whole blood was incubated with CD45-APC (BD Bioscience, Franklin Lakes, NJ) and CD41-FITC (Biolegend Catalog, San Diego, CA) for 20min at 37 °C. Samples (n = 4) were fixed with 2% paraformaldehyde for at least 30min and stored at 4 °C. Data were collected with a BD FACSCanto II (BD Biosciences, Franklin Lakes, NJ) and analyzed using the FlowJo Software (version 10.7.1). Mean fluorescent intensities are reported for all markers.

2.3.6. Biochemical assays

Plasma from downstream sampling was aliquoted and stored at −80 °C. Plasma TAT was measured using an ELISA kit from Siemens Healthineers (Erlangen, Germany). PF4 in plasma was measured using an ELISA kit from R&D Systems (Minneapolis, Minnesota). Plasma sGPVI was measured using an ELISA kit from Invitrogen (Carlsbad, California). Lastly, plasma MPO activity was measured using a fluorescent detection kit from Cell Technology (Hayward, California). All kits were run according to the manufacturers' instructions.

2.3.7. Statistics

All data are presented as mean ± standard deviation. *In vitro* data and fibrin *ex vivo* data were tested for analysis of variance (ANOVA) assumptions using Brown-Forsythe tests and quantile-quantile plots. Data sets which passed the ANOVA assumptions were tested with a 1-way ANOVA and a Tukey's *post hoc* when the main effects test was significant ($p < 0.05$). A Greenhouse–Geisser correction was used with all ANOVAs. When data sets failed an ANOVA assumption, they were tested with a Kruskal-Wallis test and a Dunn's multiple comparison test, as was the case for fibrin clotting time and FXIIa generation rate. ICP-MS, flow cytometry, and biochemical data were analyzed with 2-way ANOVAs with factors of time and metals type. TAT and PF4 data failed ANOVA assumption tests and were log transformed to allow for valid statistical analysis. Data in the manuscript are presented in their transformed version. The previously mentioned data sets were analyzed with GraphPad Prism version 10. *Ex vivo* platelet data was analyzed with

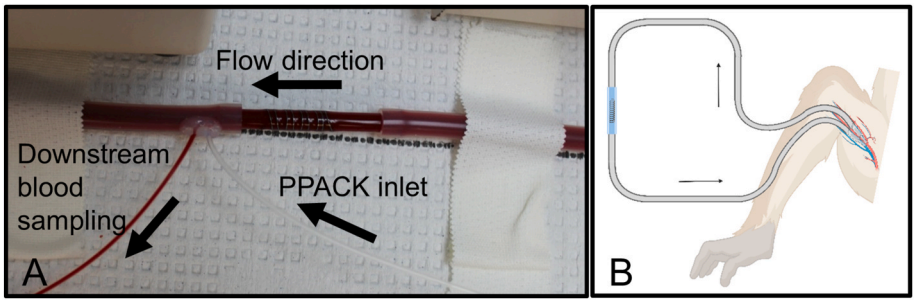

Fig. 1. Ex vivo whole blood testing on metal coils. (A) Image of a coil placed in the shunt loop showing the downstream sampling components. (B) Schematic of the non-human primate, arteriovenous shunt loop.

a repeated measures 1-way ANOVA using SPSS (IBM, version 27). No data were excluded from *in vitro* assays, platelet quantification, fibrin quantification, or flow cytometry, although PF4, MPO, and TAT data were excluded when the data did not fall within an appropriate standard range of the assay. Additionally, downstream blood plasma samples were eliminated from analysis, when they contained visible clotting which altered the sample hue.

3. Results

3.1. In vitro examination

To examine initiation and completion of the contact pathway by biodegradable and biostable metals *in vitro*, FXIIa and fibrin generation, respectively, were measured using biochemical assays with human platelet-poor plasma. Plasma only control samples were used to quantify the baseline clotting without any added material in both *in vitro* assays. The observed generation of FXIIa over time in the presence of the metal wires (Fig. 2A) showed significant differences between metal types ($p < 0.0001$). Specifically, Fe and SS had significantly higher FXIIa generation rates compared to the plasma only control. Fe, Mo, SS, CoCr, and NiTi had significantly higher FXIIa generation rates compared to the Mg wires. The fibrin generation assay also used human plasma in the presence of the metal wires to determine both the initiation time of fibrin clotting and the rate of fibrin generation. The initiation time of fibrin clotting (Fig. 2B) was significantly different between metal groups ($p < 0.0001$). Fe and Mo had a significantly lower initiation times (higher thrombogenicity) compared to the plasma only control and the Mg wires. The fibrin generation rate (Fig. 2C) also showed a significant difference ($p = 0.038$), but without any significant changes in the *post hoc* test.

3.2. Whole blood shunt study

To examine the acute thrombogenicity of the biodegradable and biostable metal wires and the measurable biomarkers present in the circulating blood downstream from the wires, this work used an *ex vivo* NHP model of flowing, whole blood without any anticoagulants. Specifically, platelet and fibrin attachment were quantified on the wires, while blood was sampled directly downstream of the wires during the 1hr testing for biochemical analysis of the plasma and platelets.

To confirm if any detectable metal degradation was present during the acute thrombogenicity testing, the downstream blood plasma samples from the flowing, whole blood were collected and analyzed with ICP-MS for Fe, Zn, Mo, and Mg ions (Supplemental Fig. 2). These results showed no significant changes in Fe, Zn, or Mo ions between any of the different pure metal types ($p = 0.959$, $p = 0.485$, $p = 0.397$, respectively). Mg ion release was significantly different ($p = 0.015$), but without any significant changes between the groups in the *post hoc* test.

These studies used whole blood *ex vivo* shunt testing without any anticoagulant or antiplatelet therapies to characterize thrombogenicity of the metal wires. All metal coils showed considerable thrombus accumulation after 1hr, except for Mg, which showed less overall accumulation of thrombosis upon visual inspection (Fig. 4A). SEM characterization of the thrombus on the wires after 1hr of testing (Fig. 3) confirmed the presence of thrombus components, including platelets, neutrophils, erythrocytes, and fibrin fibers on all wires, but with no apparent differences between metal types.

To quantify thrombogenicity on the wire coils, platelets and fibrin were radiolabeled in the whole blood testing and quantified over 1hr. Platelet and fibrin quantification (Fig. 4) on the metal wires was lower for Mg than other metals or alloys. Specifically, there were statistically fewer platelets on Mg than Mo, NiTi, or Fe metals (Fig. 4B, $p = 0.004$); however, the rate at which the platelets accumulated was not significantly different between the metal types (Fig. 4C). Fibrin accumulation (Fig. 4D) was also statistically lower on Mg than Mo, NiTi, or Fe metals ($p = 0.003$).

By collecting blood samples from immediately downstream of the wire coils, the specific markers from blood components that had interacted with the surface of the materials without attaching were analyzed. The downstream plasma TAT levels (Fig. 5A) significantly increased over time ($p < 0.0001$) but without a significant change between metal type ($p = 0.311$). Importantly, several of the downstream blood samples clotted in the draw line making some samples exceed the standard curve of the ELISAs. Specifically, there was one sample each from Fe, Mo, SS, and CoCr at 30min that showed visible clotting in the downstream sample even with the citrate and infusion of PPACK. Additionally, plasma samples from three Fe and Mg, two Mo and NiTi, and one of Zn, SS, and CoCr from the 60min time point also contained visible clots.

In addition to quantifying platelet attachment directly onto the metal

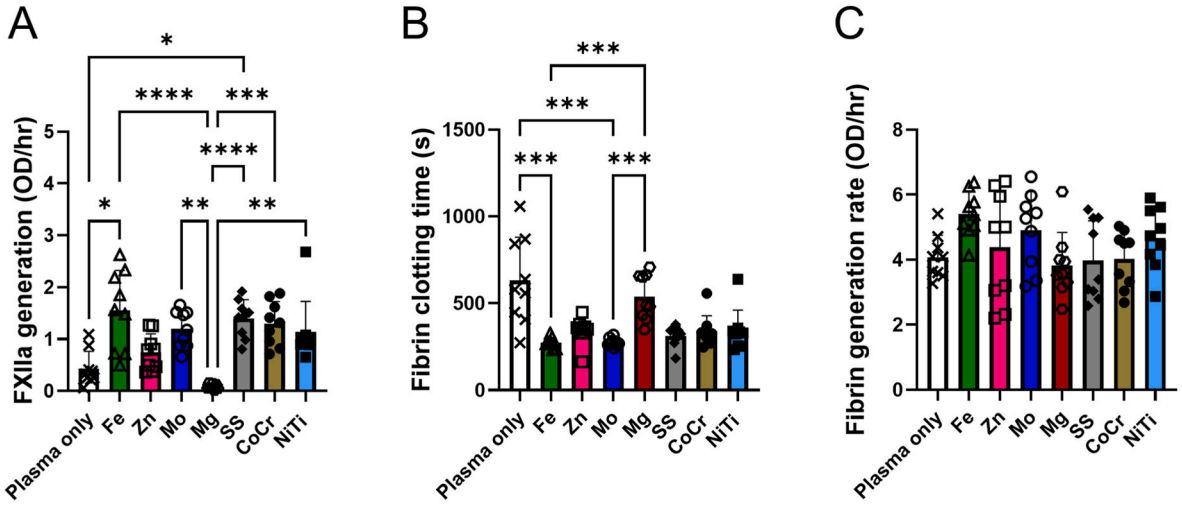

Fig. 2. In vitro analysis of human platelet-poor plasma on metal wires compared to platelet-poor plasma alone for FXIIa generation and fibrin generation assays. (A) FXIIa generation in response to Fe ($p = 0.025$) and SS ($p = 0.019$) wires was significantly higher than the plasma only control. Mg wires had a significantly less FXIIa generation compared to Fe ($p<0.0001$), Mo ($p = 0.0013$), SS ($p<0.0001$), CoCr ($p = 0.0004$), and NiTi ($p = 0.008$) wires. (B) Fibrin clotting initiation times were decreased from plasma controls, which was significant for Fe ($p = 0.0005$) and Mo ($p = 0.0006$). Mg had a significantly longer clotting time compared to Fe ($p = 0.0003$) and Mo ($p = 0.0004$). (C) Fibrin generation rate was unchanged between the metal groups and plasma negative control. * indicates $p \leq 0.05$. ** indicates $p \leq 0.01$. *** indicates $p \leq 0.001$. **** indicates $p \leq 0.0001$.

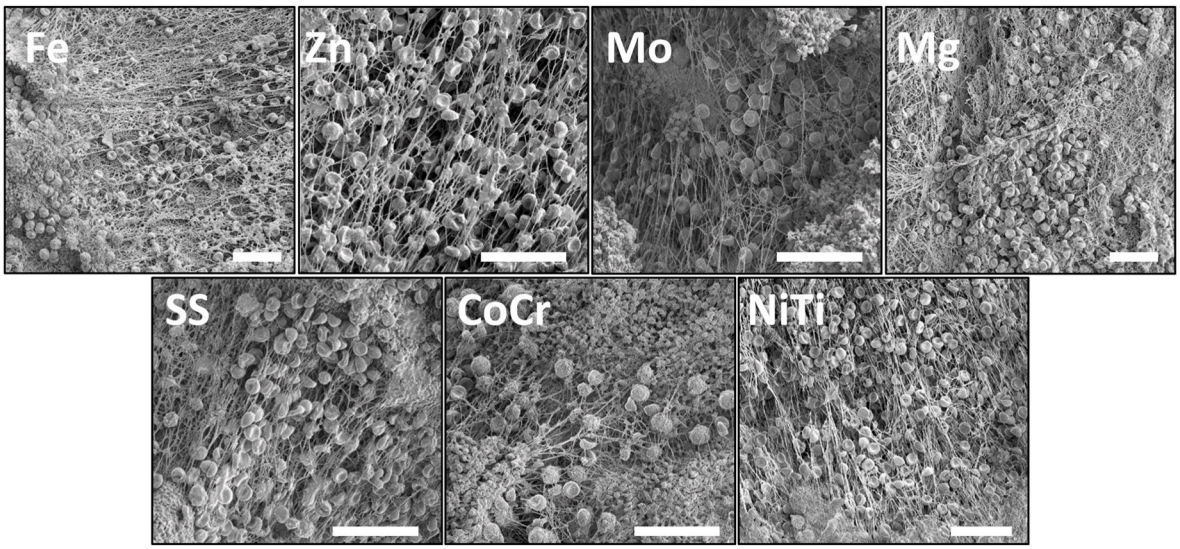

Fig. 3. Representative SEM images from wires exposed to whole flowing blood for 1hr showed thrombus elements on all samples. Scale bar = 25 μm.

coil surfaces, platelet activation markers in the plasma from the blood downstream of the metals were quantified. These downstream platelet markers in the blood samples showed no significant change in PF4 plasma concentration (Fig. 5B), sGPVI plasma concentration (Fig. 5C), or the mean fluorescent intensities of platelet surface markers of soluble P-selectin (Fig. 5D–F) between the different metal types. PF4, sGPVI, and P-selectin (at all concentrations of CRP-XL) showed a significant change over time—specifically, increasing for sGPVI, PF4, and P-selectin at 0 μg/mL CRP-XL and decreasing for P-selectin at 0.1 and 1 μg/mL CRP-XL—suggesting some platelet activation from all metal groups. While not statistically different, Fe did trend higher over time and appeared depleted in the CRP-XL-stimulated samples.

To investigate thromboinflammation within this context, MPO was quantified in the downstream blood plasma and PLAs in the downstream blood. Overall, the inflammation activation was consistent across all metal types measured through MPO activity and platelet-leukocyte interactions. Specifically, MPO (Fig. 6A) was significantly increased over time ($p < 0.0001$) but with no differences between metal type ($p = 0.811$). Platelet-leukocyte interactions (Fig. 6B) were not statistically different for either metal type ($p = 0.801$) or time ($p = 0.390$).

4. Discussion

This work characterized the thrombogenicity of pure, biodegradable metals (Fe, Zn, Mg, Mo) and alloys common in clinical cardiovascular devices (NiTi, SS, CoCr), using methods previously validated with other biomaterials [34,35]. These tests included *in vitro* quantification of FXIIa and the time to initial fibrin formation, representing the activation of the contact and common pathways of coagulation, respectively. Within downstream whole blood samples, P-selectin (protein on the surface of activated platelets) and CD41+/CD45+ ratio (defined as platelet-leukocyte interactions and marking an increase in the thromboinflammatory response) were quantified, while within downstream plasma samples the released TAT (protein complex marking net activation of coagulation), PF4 (chemokine released from activated platelets), sGPVI (soluble platelet surface marker indicative of platelet activation), and MPO (enzyme released by neutrophils indicating early inflammation activation) were quantified. Overall, the results from these measurements illustrated a dramatic reduction in the activation of the coagulation pathway from human plasma *in vitro* on Mg compared to other materials—Fe and Mo in particular. These results were replicated in a clinically relevant *ex vivo* model of flowing, whole blood in an NHP without antiplatelet or anticoagulant therapies. However, all the metals showed comparable activation of markers for platelet activation, thrombin generation, and immune responses from the blood collected downstream of the wire in the *ex vivo* model. This defines the thrombosis potential of metals that could be used in the design of biodegradable metal stents.

It is well understood that foreign materials activate the contact pathway after exposure to blood [44], which is particularly relevant to cardiovascular medical devices ranging from peripheral catheters and ports to extracorporeal membrane oxygenation (ECMO) circuits. The presence of a foreign material initiates the contact pathway, also known as the intrinsic pathway, starting with the activation of FXII to FXIIa or, more prominently, the activation of FXII by high molecular weight kininogen activating prekallikrein, which activates FXII. This pathway continues with the subsequent activation of FXI, FIX, and finally FX. Activation of FX is considered a component of the common pathway, where the intrinsic pathway meets the extrinsic pathway, the latter of which is responsible for non-pathologic clotting and hemostasis. This common pathway of coagulation produces thrombin, which converts fibrinogen to fibrin. FXII activation has been shown to be important in device-related thrombosis [38–42]. In fact, clinicians increasingly prescribe direct-acting oral anticoagulants (DOACs) to prevent activation of the coagulation pathway as a more targeted approach than dual antiplatelet therapy (DAPT, acetylsalicylic acid and clopidigrel) [45]. Most currently prescribed DOACs target thrombin or Factor X activation; however, ongoing work to block device-related thrombosis by targeting FXII and FXI with monoclonal antibodies to block their activation is ongoing and has shown efficacy in preclinical and clinical trials with ECMO and hemodialysis devices, respectively [42,46]. These therapies can prevent clotting without increased risk of bleeding. Preclinical work with monoclonal antibodies to FXII and FXI demonstrated a reduction in platelet attachment and thrombosis on nitinol stents under venous and arterial flow conditions [35]. In this work, the *in vitro* generation of FXIIa and initiation time of fibrin generation in human plasma were quantified, with *in vitro* results correlating to the *ex vivo* work, as was seen with previous biomaterial experiments [34,35]. The generation of FXIIa and reduction in the initiation of fibrin clotting time suggests that the activation of the contact pathway was initiated by all metals except Mg. The lack of activation by Mg wire (as seen in a longer fibrin clotting time and lower rate of FXIIa generation) was significant for both metrics compared to the Mo and Fe wires. However, the lack of activation of FXII by Mg did not result in a significant decrease in TAT downstream of the wires in the *ex vivo* model. While TAT did increase over time, suggesting the activation of TAT by the metals, they were not different between the

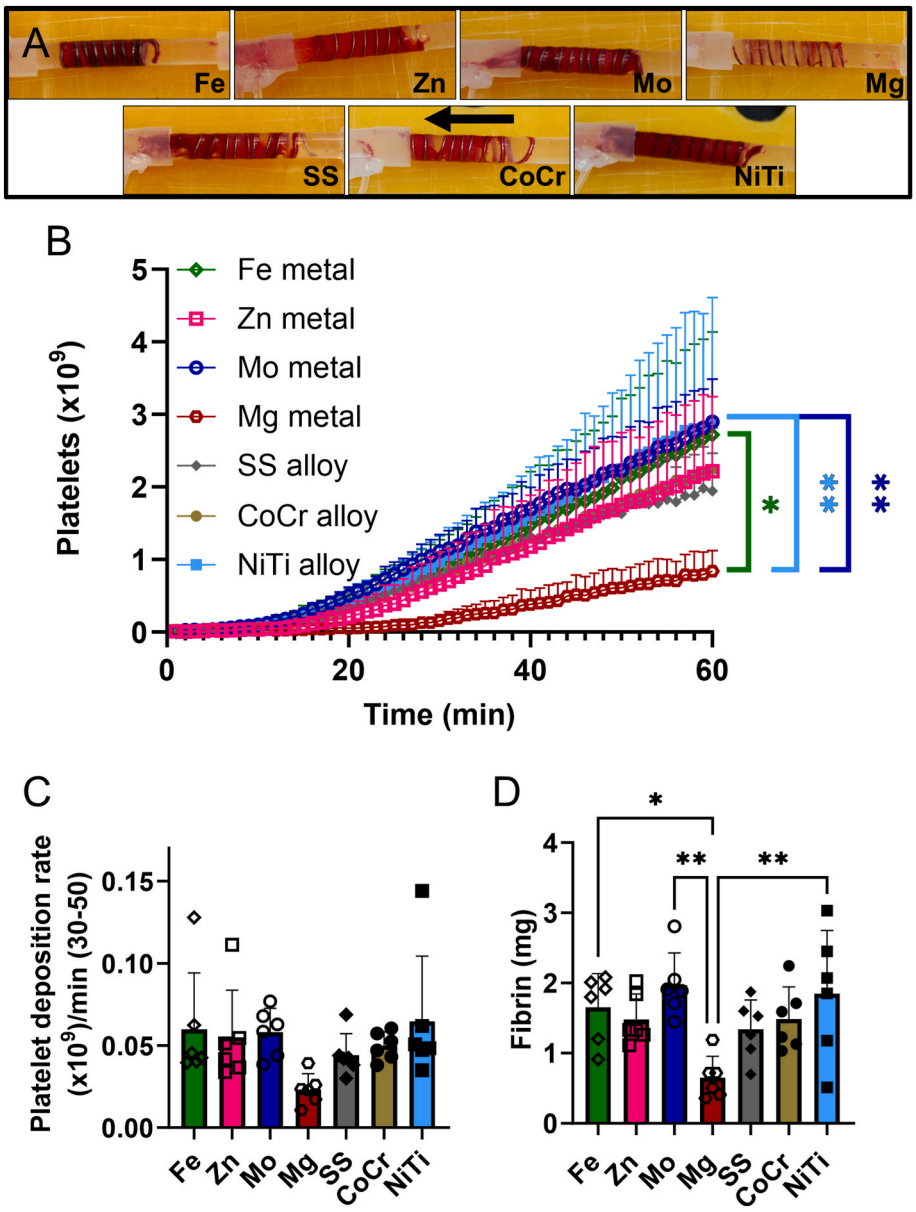

Fig. 4. Ex vivo whole blood testing. (A) Representative images of each metal coil after exposure to flowing whole blood for 1hr at 100 mL/min, with an arrow indicating the direction of blood flow. (B) Platelet attachment to metal wires, (C) rate of platelet attachment from 30 to 50 min, and (D) fibrin on pure and alloyed metal coils after 1hr exposure to flowing whole blood without anticoagulants. Platelet data were analyzed with a 1-way repeated measures ANOVA. Fibrin data were analyzed with a 1-way ANOVA. (*p<0.05, **p<0.01) Mg wires showed significantly lower platelet and fibrin accumulation compared to Fe, Mo, and NiTi.

different metal types. As these are downstream measurements, they may require longer exposure times for a difference to propagate. Alternatively, as the initiation time of thrombus formation was delayed in the shunt model, shorter time points, such as 10min intervals [41], may reveal a difference in TAT generation by Mg wires.

Platelets are a key component of a thrombus, and while they circulate in normal blood in the hundreds of billions, they are activated through signals that indicate an injury or foreign body. Platelet activation is complex and multifactorial with links to both inflammation and thrombosis, and results in the attachment, spreading, and aggregation of the platelets on cardiovascular devices. These aggregated platelets become enmeshed with erythrocytes within a fibrin network to form a thrombus, with the platelets and fibrin making up the majority of arterial thrombus composition [47]. Platelets, as well as fibrin, erythrocytes, and immune cells were seen in the surface imaging of all the metal wires after 1hr of exposure to whole, flowing blood without anticoagulant or antiplatelet interventions. The quantification of platelet attachment on the metal wires showed significantly fewer platelets on the Mg wires compared to Mo, Fe, and NiTi wires. Additionally, to characterize downstream platelet activation, these studies quantified the expression of P-selectin on platelets, and the plasma levels of sGPVI and PF4 from the blood downstream of the wire coils. In all cases, these markers increased over time, suggesting the activation of downstream platelets by the wires, but without differences between the metals. The reduction in platelet attachment on Mg and Mg alloys has been shown previously, most commonly by SEM imaging of materials after a short, static incubation in platelet-rich plasma or mechanical agitation that may not be representative of physiologic conditions [48–52]. The platelet adhesion results presented here were comparable to previous work, which used a low flow shear and fluorescent staining to demonstrate a dramatic reduction of platelet attachment on Mg alloys compared to 316L SS and L605 CoCr [53]. These studies observed limited platelet attachment and spreading on the Mg alloys, which the researchers used to conclude that many Mg alloys were

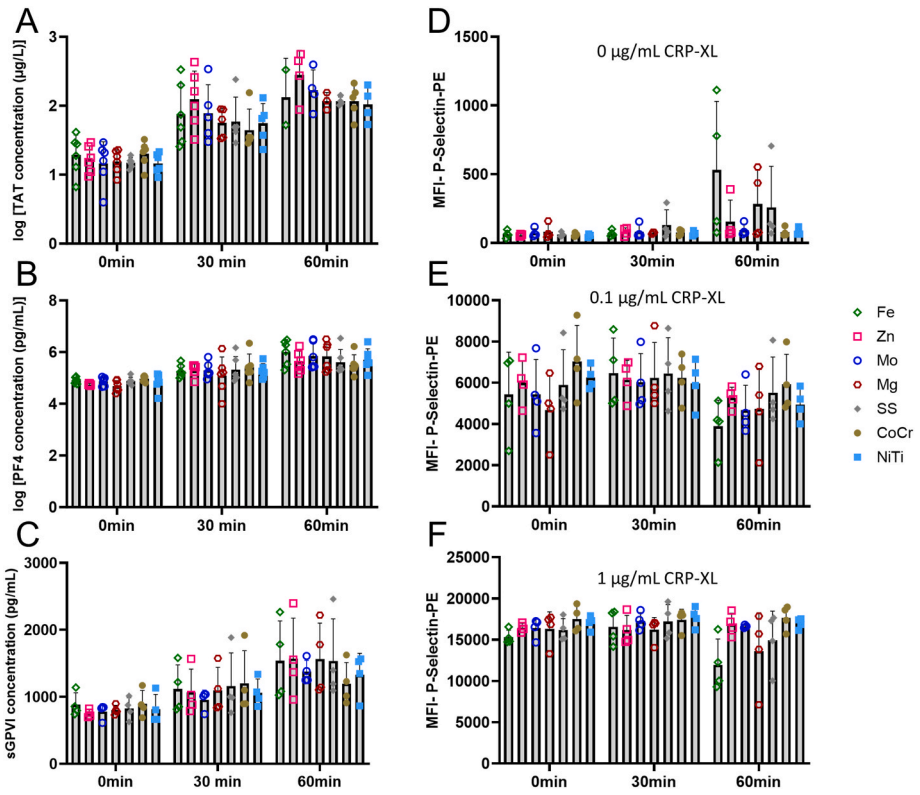

Fig. 5. Plasma samples and platelet activation collected downstream of the metal wires during *ex vivo* whole blood testing. (A) Plasma levels of TAT were measured from downstream blood sampling from the metal wires. Values significantly increased over time ($p < 0.0001$), but no change was observed between metal types ($p = 0.311$). (B) PF4 released into the blood downstream of the metal wires also showed a significant increase in PF4 released from the thrombus over time ($p < 0.0001$), but with no changes between any of the different metal wire groups ($p = 0.938$). (C) Quantification of plasma levels of sGPVI from downstream of the metal wires also showed a significant increase over time ($p < 0.0001$), but with no changes between any of the different metal wire groups ($p = 0.985$). On the platelet surface, the mean fluorescent intensities of (D) P-selectin from downstream blood without CRP-XL stimulation, (E) P-selectin with 0.1 µg/mL CRP-XL, and (F) P-selectin with 1 µg/mL CPR-XL also changed over time at all concentrations ($p = 0.008$, $p < 0.0001$, $p = 0.011$, respectively) with an increase seen over time for 0 µg/mL CRP-XL and decreases seen over time for 0.1 µg/mL CRP-XL and 1 µg/mL CRP-XL. No statistical differences were seen between the metal types for P-selectin ($p = 0.165$, $p = 0.845$, $p = 0.085$, respectively).

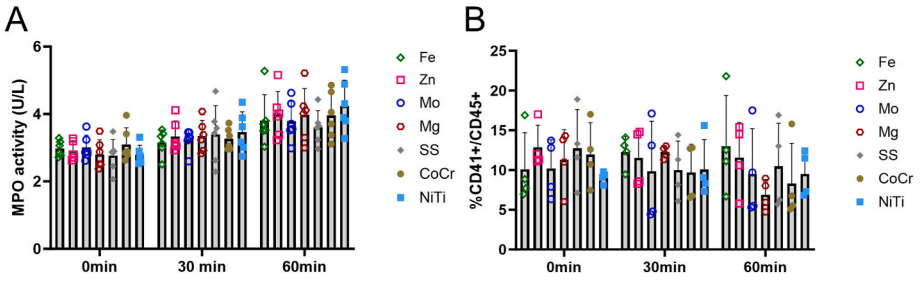

Fig. 6. Inflammation activity on plasma samples taken downstream of metals wires during *ex vivo* whole blood testing. (A) MPO released into the blood downstream of the metal wires. MPO significantly increased over time ($p < 0.0001$), but no change was observed between metal types ($p = 0.811$). (B) Platelet-leukocyte interactions from flow cytometry detection of the ratio of CD41 to CD45 in blood samples downstream of the wires. PLA was not statistically different for time ($p = 0.390$) or metal type ($p = 0.801$).

non-thrombogenic. Several of these studies and previous work have suggested that the Mg ions blocked Ca ions, which are critical for platelet activation [49,54]. In addition to the biomaterial studies cited previously, much earlier studies observed an inverse relationship to Mg concentration in the blood and platelet activation [55–57], even when blood was anticoagulated with a thrombin blocker, suggesting that platelet inhibition by Mg was independent of the clotting cascade [58]. However, this work and others' have seen that despite limiting platelet attachment, even with the strict flowing whole blood model used here, there were data to suggest that platelets were activated by the Mg surface. In a static platelet-rich plasma attachment assay, previous work found that pure Mg and Mg alloys had fewer attached platelets than CoCr; yet, their quantification of platelet activation with flow cytometry showed an increase in P-selectin from those platelets attached to the Mg-based materials, which they correlated to an increase in pH from the ions released during the Mg degradation [54]. This is comparable to the work presented here where Mg had less platelet attachment, but an increase in P-selectin from the downstream blood plasma. This downstream increase of platelet activation may be due to the increase in thrombin generation over time. It would be interesting, in future work, to examine the effects of the pH changes that occurs with Mg degradation on activated platelet and coagulation cascade proteins to decouple

the effects of pH and metal ion changes.

Overall, Mg wires caused dramatic changes with respect to platelet and fibrin attachment in the *ex vivo* model, as well as in the *in vitro* measurements of FXIIa and fibrin generation. Some preclinical and clinical data suggest that Mg can inherently inhibit human platelet activation [49,54–57]. However, these platelet-centered thrombosis studies do not explain the changes in FXIIa and fibrin generation seen in the work presented here, which utilized platelet poor plasma. Future work will be required to confirm the mechanisms involved in Mg metal prevention of FXII activation and delay of fibrin generation. Previous work with a porcine whole blood shunt model also suggested that Mg alloys have low thrombogenicity compared to SS [59], and clinical trials have shown limited thrombogenicity on Mg alloys; however, these clinical trials use antiplatelet therapies, making direct comparison challenging [60,61]. It is interesting to note the lack of differences between the types of metals that were seen for the downstream platelet, thrombosis, and inflammation markers in this work. That is, there were no significant differences between the metal types in the plasma levels of PF4, MPO, TAT from the downstream samples, as well as platelet surface measurements of platelet-leukocyte interactions or P-selectin from whole blood flow cytometry analysis. This suggests that the activation of platelets and inflammation in the blood flowing downstream of the material during this timeframe was consistent across all metal types. The observations that Mg had a lower thrombosis response, but with similar activation is important, since Mg is the most well-studied of the biodegradable metals for cardiovascular applications, including use in patients [11]. The platelet accumulation results suggested that while the Mg had lower platelet attachment, it might have been a delay in activation, since the slope of accumulation after take-off was not significantly lower. Additionally, the *in vitro* tests of fibrin generation clots showed a dramatic generation of bubbles on the Mg wires. The rapid degradation and reactivity of Mg in aqueous solution suggests that biological processes could be inhibited by the physical blocking of protein adsorption due to that rapid degradation and reactivity. While the ICP-MS data did not show detectable changes in the Mg ion concentration in the downstream plasma samples, as was expected, the gas generation may be an important biophysical process to consider when working with Mg alloys.

Previous work examining pure and binary Fe alloys noted increased platelet attachment to Fe compared to 316L SS [48], where both quiescent platelets as well as platelet aggregates were found on pure Fe [62]. In the work presented here, there were no significant differences in platelet attachment or activation on Fe compared to alloyed metals used clinically. However, platelets exposed to Fe had higher levels of surface P-selectin in the downstream blood samples, as well as a reduced granule secretion in response to platelet agonist CRP-XL, consistent with an exhausted phenotype. Previous work has shown a detrimental biological effect of pure Fe and a Fe–Mn alloy on endothelial cells and smooth muscle cells due to the generation of hydroxyl radicals as a corrosion byproduct [63,64]. This increase in oxidative stress may also explain some of the observed changes with the Fe wires, although additional studies with platelets in these extreme corrosion environments are warranted.

The understanding of corrosion rates and byproduct generation for various metals and alloys, as they relate to thrombosis, is critical for the development and design of biodegradable devices. Even though a large thrombus may not form directly on a device, downstream clotting and/or an unstable clot could nevertheless form, if a material promotes platelet activation and thrombosis. Both unstable clots and platelet activation downstream of a device increase the risk of pulmonary embolism, stroke, or myocardial infarction, which represent a huge global disease burden [65]. The results described in this work, which suggest the potential activation of platelets and coagulation by the Mg wires, as was seen in the increase of TAT, PF4, MPO, and P-selectin, indicate the need for future study of the risks of downstream platelet activation due to a Mg implant. While it is difficult to directly measure clot stability, future work may benefit from examination of the role of FXIII in addition to the fibrin quantification performed here to better understand clot stability and the risk of thromboembolism [66]. Additionally, metal ions (e.g. Zn, Fe, and Cu), which are also found endogenously in blood, have strong nitric oxide generating effects that impact many biologic responses (e.g., platelet aggregation and attachment, inflammation, smooth muscle cell proliferation and migration, endothelial cell barrier functions) and are an important area of research for biodegradable metal development [24,67–69]. However, Zn is also known to activate platelets through the GPIIBIIIA receptor [70]. While these effects were not observed in the current studies for Fe or Zn, these metal ions have the potential to improve cellular functions, which may translate to improved healing of the vascular wall and reduction of intimal hyperplasia. The ability of biodegradable metal alloys to improve biologic healing functionality supports their potential in material development, which could prevent the need for polymer-based drug coatings of questionable biocompatibility. While DES have been the standard of clinical care for many years and their ability to release drugs is powerful in altering the healing response, the polymers are strongly thrombogenic and increase the need for long-term antiplatelet and anticoagulant therapies.

The studies described here provide a comparison of blood responses in a variety of base biodegradable metals to several clinical controls using both *in vitro* and *ex vivo* assays. The ability to make these physiologically relevant comparisons in both assay types is one of the strengths of this work. Specifically, the *in vitro* work provides functional mechanistic studies by examining the time to fibrin generation and the extent of FXII activation. The former is an endpoint of the coagulation cascade, while FXII activation occurs earlier in the contact pathway of the coagulation cascade. Additionally, the *ex vivo* evaluation in a strict animal model enables the testing of the acute thrombogenicity of materials without any anticoagulant or antiplatelet therapies. This model provided both quantitative data of the primary components of arterial clotting, platelets and fibrin, and qualitative visual observations of thrombus size and composition from SEM imaging. A limitation of this study is the focus on the acute response to biomaterials only. Future work is needed to evaluate materials over the course of healing and the body's immune response, particularly with the biodegradable metals, which need thorough biological characterization throughout the degradation timeframe of 6–12 months [11,61]. However, the strict and highly thrombogenic nature of the *ex vivo* model mimics longer term thrombosis risk by eliminating the effects of anticoagulant and anti-platelet medications, which are often used in animal work. These medications reduce the understanding of the mechanisms of thrombus initiation on cardiovascular devices. Clinically, there is value in understanding thrombogenesis on cardiovascular devices with these medications, and future work should examine the role of biodegradable metals in thrombus formation under either standard antiplatelet therapies [71] or more novel DOACs [35] to gain a deeper understanding of thrombus development on stents with clinical medications.

Overall, it is important to note that even the clinical materials tested in this model were thrombogenic, illustrating the critical need for antiplatelet and antithrombotic therapies for all stents currently in use. Current coronary stent patients are prescribed 1-6mths of DAPT. Previous work using the same strict *ex vivo* thrombosis model demonstrated the dramatic reduction in platelet and fibrin attachment with DAPT [71], but given the increase in bleeding risks, clinicians will benefit from a full understanding of the thrombotic potential of any new stent materials as they consider the medication therapies of the patient after stent placement. Future work should identify the distinct mechanisms by which metals, metal ions, and metal degradation byproducts alter thrombogenesis. Additionally, future work related to research and development pursuits should consider alloying and surface modifications to generate a clinically useful device that improves hemocompatibility and reduces the necessity of antithrombotic and antiplatelet therapies. Finally, given the dominance of the contact pathway that was

seen in the results of the metals tested here, it may be valuable to look at these metals with a therapeutic targeted specifically to the contact pathway [35,42,46].

5. Conclusion

All pure and alloyed metal coils showed considerable platelet and fibrin accumulation suggesting the necessity of antiplatelet or anticoagulant therapies with clinical use and the corresponding bleeding risk that accompanies those medications. While Mg had a decreased thrombosis response in some of the results, it is unclear if this response is due to the material itself, the rapid degradation that prevents protein adsorption on the surface, and/or degradation byproducts that change the local pH. Future work will consider surface modifications and alloying to decrease thrombosis. Additionally, the contact pathway should be targeted with these materials to prevent thrombosis without the bleeding risk associated with current therapies.

Ethics approval and consent to participate

Animal studies were approved by the Oregon National Primate Research Center (ONPRC) Institutional Animal Care and Use Committee. Animals received full time care from the staff at ONPRC and work followed the guidelines from the National Research Council and the Committee on Care and Use of Laboratory Animals of the Institute of Laboratory Animal Resources.

Pooled platelet poor plasma (PPP) was isolated from healthy, human volunteers, as approved by the Oregon Health & Science University Institutional Review Board.

CRediT authorship contribution statement

D.E.J. Anderson: Writing – review & editing, Writing – original draft, Visualization, Validation, Supervision, Resources, Project administration, Methodology, Investigation, Funding acquisition, Formal analysis, Data curation. **H.H. Le:** Writing – review & editing, Writing – original draft, Visualization, Methodology, Investigation, Formal analysis, Data curation. **H. Vu:** Writing – review & editing, Writing – original draft, Methodology, Investigation, Data curation. **J. Johnson:** Writing – review & editing, Methodology, Investigation, Data curation. **J.E. Aslan:** Writing – review & editing, Writing – original draft, Supervision, Methodology, Funding acquisition, Data curation, Conceptualization. **J. Goldman:** Writing – review & editing, Writing – original draft, Supervision, Project administration, Funding acquisition, Conceptualization. **M.T. Hinds:** Writing – review & editing, Writing – original draft, Visualization, Supervision, Project administration, Methodology, Funding acquisition, Formal analysis, Data curation, Conceptualization.

Declaration of competing interest

The authors declare no conflict of interest.

Acknowledgements

This work was supported by National Institutes of Health (NIH) grants R01HL144113, R01HL101972, R01HL151367, R01HL168696, and R01HL146549. The authors gratefully acknowledge the veterinary staff at the Oregon National Primate Research Center, supported by P51OD011092. The authors also appreciate the technical consultations with Dr. Novella Keeling, Dr. Si-Han Wang, and Mr. Cole Baker. We thank Mr. Rick Mathews for his assistance in preparing this manuscript. SEM instrumentation was provided with the support of the OHSU Multiscale Microscopy Core. ICP-MS was completed at the OHSU Elemental Analysis Core, which is funded by grant S10OD028492 from the NIH. Schematic images were created with BioRender.com.

Appendix A. Supplementary data

Supplementary data to this article can be found online at https://doi.org/10.1016/j.bioactmat.2024.05.002.

References

[1] F.G. Fowkes, D. Rudan, I. Rudan, V. Aboyans, J.O. Denenberg, M.M. McDermott, P. E. Norman, U.K. Sampson, L.J. Williams, G.A. Mensah, M.H. Criqui, Comparison of global estimates of prevalence and risk factors for peripheral artery disease in 2000 and 2010: a systematic review and analysis, Lancet 382 (2013) 1329–1340.

[2] M.D. Gerhard-Herman, H.L. Gornik, C. Barrett, N.R. Barshes, M.A. Corriere, D. E. Drachman, L.A. Fleisher, F.G. Fowkes, N.M. Hamburg, S. Kinlay, R. Lookstein, S. Misra, L. Mureebe, J.W. Olin, R.A. Patel, J.G. Regensteiner, A. Schanzer, M. H. Shishehbor, K.J. Stewart, D. Treat-Jacobson, M.E. Walsh, 2016 AHA/ACC guideline on the management of patients with lower extremity peripheral artery disease: a report of the American college of cardiology/American heart association task force on clinical practice guidelines, Circulation 135 (2017) e726–e779.

[3] J.W. Olin, D.E. Allie, M. Belkin, R.O. Bonow, D.E. Casey Jr., M.A. Creager, T. C. Gerber, A.T. Hirsch, M.R. Jaff, J.A. Kaufman, C.A. Lewis, E.T. Martin, L. G. Martin, P. Sheehan, K.J. Stewart, D. Treat-Jacobson, C.J. White, Z.J. Zheng, F. A. Masoudi, R.O. Bonow, E. DeLong, J.P. Erwin 3rd, D.C. Goff Jr., K. Grady, L. A. Green, P.A. Heidenreich, K.J. Jenkins, A.R. Loth, E.D. Peterson, D.M. Shahian, F. American College of Cardiology, A. American Heart, R. American College of, I. Society for Cardiac Angiography, R. Society for Interventional, M. Society for Vascular, N. Society for Vascular, S. Society for Vascular, ACCF/AHA/ACR/SCAI/SIR/SVM/SVN/SVS 2010 performance measures for adults with peripheral artery disease: a report of the American college of cardiology foundation/American heart association task force on performance measures, the American college of radiology, the society for cardiac angiography and interventions, the society for interventional radiology, the society for vascular medicine, the society for vascular nursing, and the society for vascular surgery (writing committee to develop clinical performance measures for peripheral artery disease), J. Am. Coll. Cardiol. 56 (2010) 2147–2181.

[4] I.T. Bajeu, A.G. Niculescu, A. Scafa-Udriste, E. Andronescu, Intrastent restenosis: a comprehensive review, Int. J. Mol. Sci. 25 (2024).

[5] R. Piccolo, K.H. Bonaa, O. Efthimiou, O. Varenne, A. Baldo, P. Urban, C. Kaiser, A. de Belder, P.A. Lemos, T. Wilsgaard, J. Reifart, E.E. Ribeiro, P.W. Serruys, R. A. Byrne, J.M. de la Torre Hernandez, G. Esposito, W. Wijns, P. Juni, S. Windecker, M. Valgimigli, C. Coronary Stent Trialists, Individual patient data meta-analysis of drug-eluting versus bare-metal stents for percutaneous coronary intervention in chronic versus acute coronary syndromes, Am. J. Cardiol. 182 (2022) 8–16.

[6] K. Katsanos, S. Spiliopoulos, P. Kitrou, M. Krokidis, D. Karnabatidis, Risk of death following application of paclitaxel-coated balloons and stents in the femoropopliteal artery of the leg: a systematic review and meta-analysis of randomized controlled trials, J. Am. Heart Assoc. 7 (2018) e011245.

[7] M.T. Hawn, L.A. Graham, J.R. Richman, K.M. Itani, M.E. Plomondon, L.K. Altom, W.G. Henderson, C.L. Bryson, T.M. Maddox, The incidence and timing of noncardiac surgery after cardiac stent implantation, J. Am. Coll. Surg. 214 (2012) 658–666. ; discussion 666-657.

[8] K.D. Mahmoud, S. Sanon, E.B. Habermann, R.J. Lennon, K.M. Thomsen, D.L. Wood, F. Zijlstra, R.L. Frye, D.R. Holmes Jr., Perioperative cardiovascular risk of prior coronary stent implantation among patients undergoing noncardiac surgery, J. Am. Coll. Cardiol. 67 (2016) 1038–1049.

[9] P.K. Bowen, E.R. Shearier, S. Zhao, R.J. Guillory 2nd, F. Zhao, J. Goldman, J. W. Drelich, Biodegradable metals for cardiovascular stents: from clinical concerns to recent Zn-alloys, Adv. Healthcare Mater. 5 (2016) 1121–1140.

[10] W.J. Jang, I.H. Park, J.H. Oh, K.H. Choi, Y.B. Song, J.Y. Hahn, S.H. Choi, H. C. Gwon, C.M. Ahn, C.W. Yu, H.J. Kim, J.W. Bae, S.U. Kwon, H.J. Lee, W.S. Lee, J. O. Jeong, S.D. Park, J.H. Yang, Efficacy and safety of durable versus biodegradable polymer drug-eluting stents in patients with acute myocardial infarction complicated by cardiogenic shock, Sci. Rep. 14 (2024) 6301.

[11] A.A. Oliver, M. Sikora-Jasinska, A.G. Demir, R.J. Guillory 2nd, Recent advances and directions in the development of bioresorbable metallic cardiovascular stents: insights from recent human and in vivo studies, Acta Biomater. 127 (2021) 1–23.

[12] J. Zong, Q. He, Y. Liu, M. Qiu, J. Wu, B. Hu, Advances in the development of biodegradable coronary stents: a translational perspective, Mater Today Bio 16 (2022) 100368.

[13] T.V. Colace, G.W. Tormoen, O.J.T. McCarty, S.L. Diamond, Microfluidics and coagulation biology, Annu. Rev. Biomed. Eng. 15 (2013) 283–303.

[14] D.R. Holmes Jr., D.J. Kereiakes, S. Garg, P.W. Serruys, G.J. Dehmer, S.G. Ellis, D. O. Williams, T. Kimura, D.J. Moliterno, Stent thrombosis, J. Am. Coll. Cardiol. 56 (2010) 1357–1365.

[15] C. Negrier, Y. Dargaud, J.C. Bordet, Basic aspects of bypassing agents, Haemophilia 12 (Suppl 6) (2006) 48–52. ; discussion 52-43.

[16] T. Palmerini, G. Biondi-Zoccai, D. Della Riva, A. Mariani, P. Genereux, A. Branzi, G. W. Stone, Stent thrombosis with drug-eluting stents: is the paradigm shifting? J. Am. Coll. Cardiol. 62 (2013) 1915–1921.

[17] R.W. Yeh, D.J. Kereiakes, P.G. Steg, S. Windecker, M.J. Rinaldi, A.H. Gershlick, D. E. Cutlip, D.J. Cohen, J.F. Tanguay, A. Jacobs, S.D. Wiviott, J.M. Massaro, A. C. Iancu, L. Mauri, D.S. Investigators, Benefits and risks of extended duration dual antiplatelet therapy after PCI in patients with and without acute myocardial infarction, J. Am. Coll. Cardiol. 65 (2015) 2211–2221.

[18] R. Yanagisawa, K. Hayashida, Y. Yamada, M. Tanaka, F. Yashima, T. Inohara, T. Arai, T. Kawakami, Y. Maekawa, H. Tsuruta, Y. Itabashi, M. Murata, M. Sano, K. Okamoto, A. Yoshitake, H. Shimizu, M. Jinzaki, K. Fukuda, Incidence, predictors, and mid-term outcomes of possible leaflet thrombosis after TAVR, JACC Cardiovasc Imaging (2016).
[19] B. Tillman, D. Gailani, Inhibition of factors XI and XII for prevention of thrombosis induced by artificial surfaces, Semin. Thromb. Hemost. (2017).
[20] J. Casan, R.K. Andrews, E.E. Gardiner, A.K. Davis, Mechanisms of platelet dysfunction in patients with implantable devices, Semin. Thromb. Hemost. 44 (2018) 12–19.
[21] A. Martins Lima, A.C. Martins Cavaco, R.A. Fraga-Silva, J.A. Eble, N. Stergiopulos, From patients to platelets and back again: pharmacological approaches to glycoprotein VI, a thrilling antithrombotic target with minor bleeding risks, Thromb. Haemostasis 119 (2019) 1720–1739.
[22] S.M. Modi K, K. Mahajan, Stent Thrombosis, StatPearls [Internet], StatPearls Publishing, Treasure Island (FL), 2023.
[23] J.W. Drelich, J. Goldman, Bioresorbable vascular metallic scaffolds: current status and research trends, Current Opinion in Biomedical Engineering 24 (2022) 100411.
[24] C.W. McCarthy, R.J. Guillory, J. Goldman, M.C. Frost, Transition-metal-Mediated release of nitric oxide (NO) from S-nitroso-N-acetyl-d-penicillamine (SNAP): potential applications for endogenous release of NO at the surface of stents via corrosion products, ACS Appl. Mater. Interfaces 8 (2016) 10128–10135.
[25] J.S. Lee, Nanopore analysis of the effect of metal ions on the folding of peptides and proteins, Protein Pept. Lett. 21 (2014) 247–255.
[26] R.J. Guillory 2nd, T.M. Kolesar, A.A. Oliver, J.A. Stuart, M.L. Bocks, J.W. Drelich, J. Goldman, Zn(2+)-dependent suppression of vascular smooth muscle intimal hyperplasia from biodegradable zinc implants, Mater. Sci. Eng., C 111 (2020) 110826.
[27] R.J. Guillory 2nd, E. Mostaed, A.A. Oliver, L.M. Morath, E.J. Earley, K.L. Flom, T. M. Kolesar, A. Mostaed, H.D. Summers, M.P. Kwesiga, J.W. Drelich, K.D. Carlson, D. Dragomir-Daescu, J. Goldman, Improved biocompatibility of Zn-Ag-based stent materials by microstructure refinement, Acta Biomater. 145 (2022) 416–426.
[28] A.A. Oliver, R.J. Guillory 2nd, K.L. Flom, L.M. Morath, T.M. Kolesar, E. Mostaed, M. Sikora-Jasinska, J.W. Drelich, J. Goldman, Analysis of vascular inflammation against bioresorbable Zn-Ag based alloys, ACS Appl. Bio Mater. 3 (2020) 6779–6789.
[29] S. Zhao, J.M. Seitz, R. Eifler, H.J. Maier, R.J. Guillory 2nd, E.J. Earley, A. Drelich, J. Goldman, J.W. Drelich, Zn-Li alloy after extrusion and drawing: structural, mechanical characterization, and biodegradation in abdominal aorta of rat, Mater. Sci. Eng., C 76 (2017) 301–312.
[30] P.K. Bowen, J.M. Seitz, R.J. Guillory 2nd, J.P. Braykovich, S. Zhao, J. Goldman, J. W. Drelich, Evaluation of wrought Zn-Al alloys (1, 3, and 5 wt % Al) through mechanical and in vivo testing for stent applications, J. Biomed. Mater. Res. B Appl. Biomater. 106 (2018) 245–258.
[31] R.J. Guillory 2nd, A.A. Oliver, E. Davis, E.J. Earley, J.W. Drelich, J. Goldman, Preclinical in-vivo evaluation and screening of zinc based degradable metals for endovascular stents, JOM 71 (2019) 1436–1446, 1989.
[32] R.J. Guillory 2nd, M. Sikora-Jasinska, J.W. Drelich, J. Goldman, In vitro corrosion and in vivo response to zinc implants with electropolished and anodized surfaces, ACS Appl. Mater. Interfaces 11 (2019) 19884–19893.
[33] G. Katarivas Levy, A. Kafri, Y. Ventura, A. Leon, R. Vago, J. Goldman, E. Aghion, Surface stabilization treatment enhances initial cell viability and adhesion for biodegradable zinc alloys, Mater. Lett. 248 (2019) 130–133.
[34] M.E. Fallon, H.H. Le, N.M. Bates, Y. Yao, E.K.F. Yim, M.T. Hinds, D.E.J. Anderson, Hemocompatibility of micropatterned biomaterial surfaces is dependent on topographical feature size, Front. Physiol. 13 (2022) 983187.
[35] N.M. Keeling, M. Wallisch, J. Johnson, H.H. Le, H.H. Vu, K.R. Jordan, C. Puy, E. I. Tucker, K.P. Nguyen, O.J.T. McCarty, J.E. Aslan, M.T. Hinds, D.E.J. Anderson, Pharmacologic targeting of coagulation factors XII and XI by monoclonal antibodies reduces thrombosis in nitinol stents under flow, J. Thromb. Haemostasis (2024).
[36] O.J. McCarty, Y. Zhao, N. Andrew, L.M. Machesky, D. Staunton, J. Frampton, S. P. Watson, Evaluation of the role of platelet integrins in fibronectin-dependent spreading and adhesion, J. Thromb. Haemostasis 2 (2004) 1823–1833.
[37] D.E.J. Anderson, J.J. Glynn, H.K. Song, M.T. Hinds, Engineering an endothelialized vascular graft: a rational approach to study design in a non-human primate model, PLoS One 9 (2014) e115163.
[38] D.E.J. Anderson, K.P. Truong, M.W. Hagen, E.K.F. Yim, M.T. Hinds, Biomimetic modification of poly(vinyl alcohol): encouraging endothelialization and preventing thrombosis with antiplatelet monotherapy, Acta Biomater. (2019).
[39] M.F. Cutiongco, D.E. Anderson, M.T. Hinds, E.K. Yim, In vitro and ex vivo hemocompatibility of off-the-shelf modified poly(vinyl alcohol) vascular grafts, Acta Biomater. 25 (2015) 97–108.
[40] Y. Yao, A.M. Zaw, D.E.J. Anderson, Y. Jeong, J. Kunihiro, M.T. Hinds, E.K.F. Yim, Fucoidan and topography modification improved in situ endothelialization on acellular synthetic vascular grafts, Bioact. Mater. 22 (2023) 535–550.
[41] E.I. Tucker, U.M. Marzec, T.C. White, S. Hurst, S. Rugonyi, O.J.T. McCarty, D. Gailani, A. Gruber, S.R. Hanson, Prevention of vascular graft occlusion and thrombus-associated thrombin generation by inhibition of factor XI, Blood 113 (2009) 936–944.
[42] M. Wallisch, C.U. Lorentz, H.H.S. Lakshmanan, J. Johnson, M.R. Carris, C. Puy, D. Gailani, M.T. Hinds, O.J.T. McCarty, A. Gruber, E.I. Tucker, Antibody inhibition of contact factor XII reduces platelet deposition in a model of extracorporeal membrane oxygenator perfusion in nonhuman primates, Research and Practice in Thrombosis and Haemostasis 4 (2020) 205–216.
[43] S. Rugonyi, E. Tucker, U. Marzec, A. Gruber, S. Hanson, Transport-reaction model of mural thrombogenesis: comparisons of mathematical model predictions and results from baboon models, Ann. Biomed. Eng. 38 (2010) 2660–2675.
[44] S.R. Hanson, E.I. Tucker, R.A. Latour, 2.2.6 - blood coagulation and blood–material interactions, in: W.R. Wagner, S.E. Sakiyama-Elbert, G. Zhang, M.J. Yaszemski (Eds.), Biomaterials Science, fourth ed., Academic Press, 2020, pp. 801–812.
[45] S. Julia, U. James, Direct oral anticoagulants: a quick guide, Eur. Cardiol. 12 (2017) 40–45.
[46] C.U. Lorentz, E.I. Tucker, N.G. Verbout, J.J. Shatzel, S.R. Olson, B.D. Markway, M. Wallisch, M. Ralle, M.T. Hinds, O.J.T. McCarty, D. Gailani, J.I. Weitz, A. Gruber, The contact activation inhibitor AB023 in heparin-free hemodialysis: results of a randomized phase 2 clinical trial, Blood 138 (2021) 2173–2184.
[47] I.N. Chernysh, C. Nagaswami, S. Kosolapova, A.D. Peshkova, A. Cuker, D.B. Cines, C.L. Cambor, R.I. Litvinov, J.W. Weisel, The distinctive structure and composition of arterial and venous thrombi and pulmonary emboli, Sci. Rep. 10 (2020) 5112.
[48] B. Liu, Y.F. Zheng, Effects of alloying elements (Mn, Co, Al, W, Sn, B, C and S) on biodegradability and in vitro biocompatibility of pure iron, Acta Biomater. 7 (2011) 1407–1420.
[49] A. Mochizuki, H. Kaneda, Study on the blood compatibility and biodegradation properties of magnesium alloys, Mater. Sci. Eng., C 47 (2015) 204–210.
[50] X. Gu, Y. Zheng, Y. Cheng, S. Zhong, T. Xi, In vitro corrosion and biocompatibility of binary magnesium alloys, Biomaterials 30 (2009) 484–498.
[51] T.Y. Nguyen, A.F. Cipriano, R.G. Guan, Z.Y. Zhao, H. Liu, In vitro interactions of blood, platelet, and fibroblast with biodegradable magnesium-zinc-strontium alloys, J. Biomed. Mater. Res. 103 (2015) 2974–2986.
[52] N. Zhao, N. Watson, Z. Xu, Y. Chen, J. Waterman, J. Sankar, D. Zhu, In vitro biocompatibility and endothelialization of novel magnesium-rare Earth alloys for improved stent applications, PLoS One 9 (2014) e98674.
[53] C. Hansi, A. Arab, A. Rzany, I. Ahrens, C. Bode, C. Hehrlein, Differences of platelet adhesion and thrombus activation on amorphous silicon carbide, magnesium alloy, stainless steel, and cobalt chromium stent surfaces, Cathet. Cardiovasc. Interv. 73 (2009) 488–496.
[54] C. Yahata, A. Mochizuki, Platelet compatibility of magnesium alloys, Mater. Sci. Eng., C 78 (2017) 1119–1124.
[55] W.L. Leaphart, M.C. Meyer, E.L. Capeless, P.B. Tracy, Adenosine diphosphate-induced platelet activation inhibited by magnesium in a dose-dependent manner, Obstet. Gynecol. 91 (1998) 421–425.
[56] M. Shechter, C.N. Merz, R.K. Rude, M.J. Paul Labrador, S.R. Meisel, P.K. Shah, S. Kaul, Low intracellular magnesium levels promote platelet-dependent thrombosis in patients with coronary artery disease, Am. Heart J. 140 (2000) 212–218.
[57] D.L. Hwang, C.F. Yen, J.L. Nadler, Effect of extracellular magnesium on platelet activation and intracellular calcium mobilization, Am. J. Hypertens. 5 (1992) 700–706.
[58] H.B. Ravn, S.D. Kristensen, H. Vissinger, S.E. Husted, Magnesium inhibits human platelets, Blood Coagul. Fibrinolysis 7 (1996) 241–244.
[59] M.J. Lipinski, E. Acampado, Q. Cheng, L. Adams, S. Torii, J. Gai, R. Torguson, D. G. Hellinga, M. Joner, C. Harder, P. Zumstein, A.V. Finn, F.D. Kolodgie, R. Virmani, R. Waksman, Comparison of acute thrombogenicity for magnesium versus stainless steel stents in a porcine arteriovenous shunt model, EuroIntervention 14 (2019) 1420–1427.
[60] M. Sabate, F. Alfonso, A. Cequier, S. Romani, P. Bordes, A. Serra, A. Iniguez, P. Salinas, B. Garcia Del Blanco, J. Goicolea, R. Hernandez-Antolin, J. Cuesta, J. A. Gomez-Hospital, L. Ortega-Paz, J. Gomez-Lara, S. Brugaletta, Magnesium-based resorbable scaffold versus permanent metallic sirolimus-eluting stent in patients with ST-segment elevation myocardial infarction: the MAGSTEMI randomized clinical trial, Circulation 140 (2019) 1904–1916.
[61] A.A. Oliver, K.D. Carlson, C. Bilgin, J.L. Arturo Larco, R. Kadirvel, R. J. Guillory 2nd, D. Dragomir Daescu, D.F. Kallmes, Bioresorbable flow diverters for the treatment of intracranial aneurysms: review of current literature and future directions, J. Neurointerventional Surg. 15 (2023) 178–182.
[62] F.L. Nie, Y.F. Zheng, S.C. Wei, C. Hu, G. Yang, In vitro corrosion, cytotoxicity and hemocompatibility of bulk nanocrystalline pure iron, Biomed Mater 5 (2010) 065015.
[63] E. Scarcello, A. Herpain, M. Tomatis, F. Turci, P.J. Jacques, D. Lison, Hydroxyl radicals and oxidative stress: the dark side of Fe corrosion, Colloids Surf. B Biointerfaces 185 (2020) 110542.
[64] E. Scarcello, I. Lobysheva, C. Bouzin, P.J. Jacques, D. Lison, C. Dessy, Endothelial dysfunction induced by hydroxyl radicals - the hidden face of biodegradable Fe-based materials for coronary stents, Mater. Sci. Eng., C 112 (2020) 110938.
[65] G.B.D. Diseases, C. Injuries, Global burden of 369 diseases and injuries in 204 countries and territories, 1990-2019: a systematic analysis for the Global Burden of Disease Study 2019, Lancet 396 (2020) 1204–1222.
[66] A.S. Wolberg, Y. Sang, Fibrinogen and factor XIII in venous thrombosis and thrombus stability, Arterioscler. Thromb. Vasc. Biol. 42 (2022) 931–941.
[67] I. Russo, C. Barale, E. Melchionda, C. Penna, P. Pagliaro, Platelets and cardioprotection: the role of nitric oxide and carbon oxide, Int. J. Mol. Sci. 24 (2023).
[68] N.D. Tsihlis, C.S. Oustwani, A.K. Vavra, Q. Jiang, L.K. Keefer, M.R. Kibbe, Nitric oxide inhibits vascular smooth muscle cell proliferation and neointimal hyperplasia by increasing the ubiquitination and degradation of UbcH10, Cell Biochem. Biophys. 60 (2011) 89–97.

[69] T.J. Guzik, R. Korbut, T. Adamek-Guzik, Nitric oxide and superoxide in inflammation and immune regulation, J. Physiol. Pharmacol. 54 (2003) 469–487.
[70] P. Heyns Adu, A. Eldor, R. Yarom, G. Marx, Zinc-induced platelet aggregation is mediated by the fibrinogen receptor and is not accompanied by release or by thromboxane synthesis, Blood 66 (1985) 213–219.
[71] M.W. Hagen, G. Girdhar, J. Wainwright, M.T. Hinds, Thrombogenicity of flow diverters in an ex vivo shunt model: effect of phosphorylcholine surface modification, J. Neurointerventional Surg. 9 (2017) 1006–1011.